

RECENT PROGRESS OF THE BEAM COMMISSIONING IN J-PARC LINAC

T. Maruta*, Y. Liu, K. Futatsukawa, T. Miyao, KEK, Tsukuba, Japan
 M. Ikegami, FRIB, East Lansing, MI, USA
 A. Miura, JAEA, Tokai-mura, Japan

Abstract

The injector linac of Japan Proton Accelerator Research Complex (J-PARC) is recently conducted a front-end upgrade to increase the feasible peak current to 50 mA. Together with the beam energy upgrade in year 2013, we are ready for challenge into design beam power of 1 MW operation at the 3 GeV Rapid Cycling Synchrotron (RCS). The 1st commissioning after the upgrade began at September 29th, and then we successfully realized 50 mA beam acceleration on October 15th. In this paper, recent progress of linac beam commissioning, especially for after the front-end upgrade is described.

INTRODUCTION

J-PARC is a MW-class multi purpose proton accelerator facility in Japan. The accelerator is comprised from a 400 MeV linac, a 3 GeV RCS and a 50 GeV main ring (MR). The MR is currently operating at 30 GeV. The linac consists of 50 keV negative hydrogen (H^-) ion source (IS), a 3 MeV Radio Frequency Quadrupole (RFQ), a 50 MeV Drift Tube Linac (DTL), an 191 MeV Separate-type DTL (SDTL) and a 400 MeV Annular-ring Coupled Structure (ACS) linac as shown in Fig.1 [1]. There are three beam transport sections; MEBT1 is between RFQ and DTL, MEBT2 is in SDTL and ACS and L3BT is from ACS to 3 GeV RCS, respectively. The RF frequency is 324 MHz in RFQ, DTL and SDTL, and ACS is threefold frequency of 972 MHz.

Outline of the Linac Upgrade

In the linac, a beam power upgrade project had been conducted in year 2013 - 2014 to achieve the design beam power of 1 MW at the RCS extraction. Before this upgrade, the beam energy and the peak current were 181 MeV and 30 mA, respectively. The upgrade is divided in two periods. The 1st period is a beam energy upgrade from 181 MeV to 400 MeV by introducing ACS after the existing linac. The aim of this upgrade is the alleviation of the Laslett incoherent tune shift at RCS. Since the shift amount is inversely proportional to $\beta^2\gamma^3$ (β, γ : Lorentz factor), This energy extension reduces the shift amount to be $< 1/3$, and it is settled in an acceptable range even in 50 mA.

In the 2nd period of the intensity upgrade, the IS is replaced to an RF-driven type and RFQ (RFQ III) is also replaced to new one which is designed for 50 mA. To handle the higher beam power from the RFQ III, we also upgraded the RF chopper system placed in MEBT1; introduction of a tandem scraper configuration and new chopper cavity.

* tmaruta@post.j-parc.jp

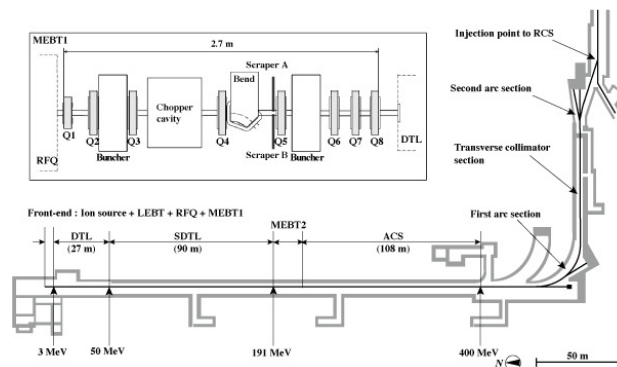


Figure 1: Outline of the J-PARC linac. The top-left Figure is the detail of MEBT1 between RFQ and DTL.

PROGRESS OF THE COMMISSIONING

The linac beam commissioning after the intensity upgrade began at September 29th, and continues till October 14th. There are main purposes; establishment of 400 MeV accelerator, a 50 mA tuning for a high power test and a 30 mA tuning for an user operation. We successfully accelerate a 50 mA beam at October 14th. In this section, the progress of the linac beam commissioning after the front-end upgrade is discussed.

MEBT1 Matching

It is needless to say that the replacement of the front-end results a variation of the beam distribution at RFQ exit, and this variation must be absorbed in MEBT1. Moreover, MEBT1 is the most severe matching section from the point of view of space-charge force due to its low energy. Therefore, an accurate matching is required for a beam halo mitigation. We firstly measured a transverse beam profile in MEBT1 by Q-scan. Then, the MEBT1 optics was determined from this measurement and simulated longitudinal profile at the RFQ III by PARMTEQM [2]. After setting a new lattice, we conducted a DTL acceptance scan [3] to check the consistency for longitudinal profile. We also measured a transverse beam profile at the SDTL entrance, because the beam profile at this region strongly depends on the accuracy of the MEBT1 matching.

The Q-scan is conducted by Q3 and the wire scanner monitor (WSM) between the RF chopper cavity and Q4 which is 0.62 m downstream from Q3. Since we turn off the chopper RF while a measurement, the lattice between them is quadrupole + drift. In the thin lens approximation, the square of beam size at the WSM (σ_{WSM}^2) is a 2nd order polynomial function described from the Twiss parameter at

Content from this work may be used under the terms of the CC BY 3.0 licence (© 2015). Any distribution of this work must maintain attribution to the author(s), title of the work, publisher, and DOI.

Q3 (α_{Q3}, β_{Q3} and γ_{Q3}), emittance (ϵ), drift length (L) and Q3 gradient (k) as,

$$\sigma_{WSM}^2 = \epsilon \left[(1 + Lk)^2 \beta_{Q3} - 2(1 + Lk)L\alpha_{Q3} + L^2\gamma_{Q3} \right]. \quad (1)$$

The beam profile is measured at 14 different Q3 gradients. We fit the measurement and then calculate the Twiss parameter at the Q3 by TRACE3D [4] in which linear space-charge impulse is included. And then, the obtained Twiss parameter at Q3 is extrapolated to the RFQ III exit for a comparison it with a RFQ simulation.

Table 1: Summary of Transverse Beam Profile at the MEBT1 Entrance

	Simulation	Measurement	
	50 mA	30 mA	50 mA
α_x	-1.49	-1.32	-1.27
α_y	1.54	0.59	0.99
β_x (mm/mrad)	0.300	0.180	0.208
β_y (mm/mrad)	0.212	0.088	0.132
ϵ_x ($\pi \cdot \text{mm} \cdot \text{mrad}$)	0.264	0.277	0.281
ϵ_x ($\pi \cdot \text{mm} \cdot \text{mrad}$)	0.264	0.256	0.321

Table 1 shows the summary of transverse Twiss parameter at the RFQ III exit at peak current of 30 mA and 50 mA. The ellipses on both horizontal (x) and vertical (y) phase spaces are also shown in Fig. 2. The simulated Twiss parameter is also shown for a comparison. While the simulated ellipse is almost mirror symmetry in x and y phase space, the vertical ellipse is steeper than the horizontal one in the measurement. The emittance in 30 mA is almost same as simulated 50 mA one. The measured emittance in 50 mA is about 10% bigger than 30 mA one.

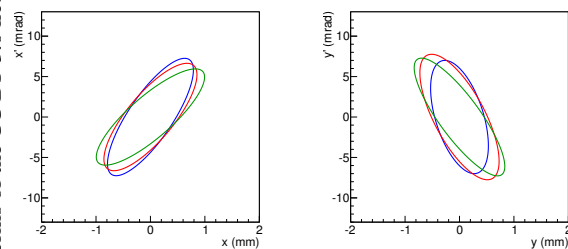


Figure 2: The top Figure shows the DTL longitudinal acceptance (pale blue) and micro particle distribution in design (red). The bottom Figure is the DTL acceptance scan.

Concerning to the longitudinal beam profile, we employed a simulated Twiss parameters by PARMTEQM due to lack of longitudinal beam monitor. After the determination of the MEBT1 optics, we conducted a DTL acceptance scan to check the consistency of the simulation and reality.

The top Figure of Fig. 3 shows the simulated DTL longitudinal acceptance (pale blue) and design beam profile (red). The acceptance and the beam distribution is simulated by 3D Particle-in-Cell code IMPACT [5]. In the design, micro

particles are well inside of the acceptance. If we gradually shift the DTL acceptance to phase direction by changing the driving phase of all DTL cavities with same amount, the beam bunch also shifts from the acceptance center. And then, the peripheral particles spill from the acceptance. Since the particles out of the acceptance do not accelerate by DTL, these particles are finally lost in the middle of the beam line due to the mismatch of transverse focus. This situation is equivalent to the transverse profile measurement by beam collimation with a one-side movable jaw. The beam transmission declines as the acceptance shift being large because the particles out of the acceptance increase. The shape of decline curve depends on the beam bunch at the DTL entrance. The measurement of the decline curve gives us a hint of longitudinal beam profile.

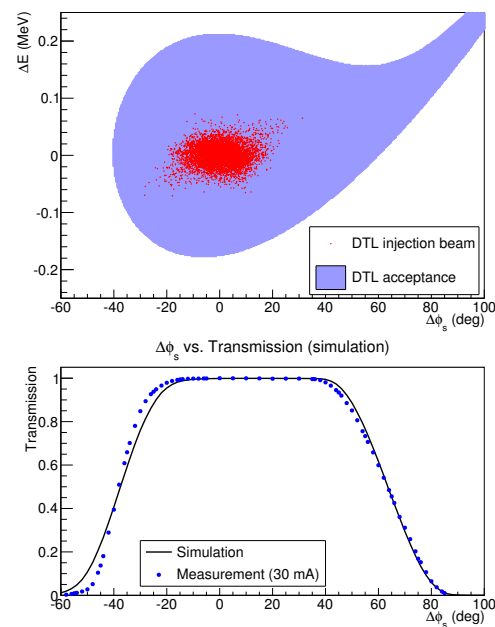


Figure 3: The top Figure shows the DTL longitudinal acceptance (pale blue) and micro particle distribution in design (red). The bottom Figure is the DTL acceptance scan.

The bottom figure of Fig. 3 shows a result of DTL acceptance scan measurement and a simulation for comparison. Whereas the decline curve at positive phase looks similar, the measured curve is steeper than the simulation in negative phase. The acceptance edge at negative phase is almost perpendicular to a phase axis. The actual beam size on phase axis is considered to be narrower than the design. In the present optics, there is an imperfection in longitudinal matching, and we need further study for an improvement.

After the setting of new MEBT1 optics, we measured transverse beam profile at the SDTL entrance by WSMs. The imperfection of MEBT1 matching causes a beam halo generation. Even if the imperfection of the longitudinal phase space, the transverse halo could appear due to space charge oriented transverse and longitudinal coupling. Therefore, the transverse beam profile is important probe to check

the perfection of the MEBT1 matching. Typical beam profiles at the SDTL entrance in 30 mA and 50 mA are shown in Fig. 4. The left and right Figures are horizontal and vertical distributions, respectively. These profiles are measured by the WSM which locates between 3rd and 4th SDTL cavities. Since the dynamic range of the WSM is in order of 10^4 , the fluctuation around 10^{-4} range is noise. Whereas no beam halo component is observed in 30 mA, the shoulders in 10^{-2} are seen in 50 mA. It means there is an imperfection in 50 mA matching. We need further study to polish up the matching.

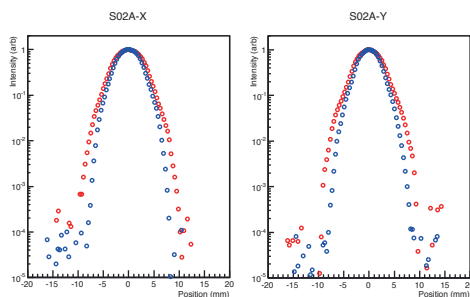


Figure 4: Horizontal (left) and vertical (right) beam profiles at the SDTL entrance. Blue and red points are in 30 mA and 50 mA, respectively. The signal in 10^{-4} is noise.

Transverse Emittance and Beam Loss

Figure 5 shows the transverse emittance measurements in all matching sections. Emittance growth are seen between MEBT1 to SDTL, but no growth occurs after SDTL. This growth is also observed in an IMPACT simulation, and is because of the long distance of focusing periods in MEBT1. If we compare these emittances with that at 25 mA with a previous front-end, the 30 mA emittance are almost comparable. It should be noticed that the emittance at RFQ exit in the previous front-end is 30 % smaller than that of the new front-end. Therefore, the matching accuracy is considered to be much improved in this commissioning.

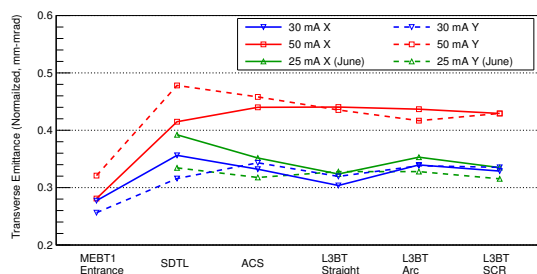


Figure 5: Measured transverse emittance at 30 mA (blue) and 50 mA (red) in all matching sections, the emittance in 25 mA with a previous front-end is drawn for a comparison.

The highest residual radiation in the linac is observed in ACS. We measure the beam loss in 30 mA and 50 mA, and compare them by scaling the signals by peak current (BLM at 30mA x 50/30) as shown in Fig. 6. 50 mA signal and scaled

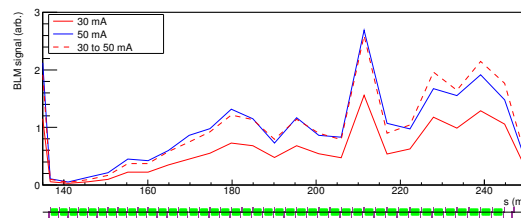


Figure 6: BLM signal comparison in the ACS section. The BLM signals were measured in 30 mA (red, solid line) and 50 mA (blue, solid line). The 30 mA signals scaled by 50/30 (red, dashed line) is also drawn for a comparison.

30 mA signal are well consistent. At present, The beam power in user operation is 500 kW at the RCS extraction. We have observed more than 2 mSv/h on chamber surfaces in ACS after 5 hours from a beam operation. Therefore, the reduction of the beam loss is a crucial issue for the linac. One of the major source of the beam loss is beam stripping (IBSt) [6]. However the IBSt is proportional to square of peak current, the larger emittance in 50 mA than 30 mA makes almost linear correlation of the beam loss. Recently we are quantitatively investigating the IBSt [7].

SUMMARY AND PROSPECTS

We successfully accelerate the 50 mA beam at October 15th 2014 in the 1st beam commissioning after the front-end upgrade. In the present user operation, we stably supplies a 30 mA beam to RCS, which is equivalent to 500 kW at the RCS extraction. Concerning to the beam profile in SDTL, the matching in MEBT1 looks very well in 30 mA. However, there are significant beam halos in 50 mA. We consider that an imperfection exists in the MEBT1 matching in 50 mA. We need further study to improve the beam quality, especially understanding of longitudinal beam profile is important. Toward to the stable operation in design beam power, we continue the beam study.

REFERENCES

- [1] Y. Yamazaki eds., "Technical design report of J- PARC", KEK Report 2002-13, JAERI-Tech 2003- 44.
- [2] K.R.Crandall,et. al., "RFQ Design Codes", LANL Report, LA-UR-96-1836 (1996).
- [3] T. Maruta et. al., Proceedings of 2nd International Particle Accelerator Conference (IPAC11), San Sebastian, Spain, September 4 - 9, 2011. pp. 2592 - 2594.
- [4] K.R. Crandall, "TRACE: An Interactive Beam Dynamics Code", in Linear Accelerator and Beam Optics Codes", ed. Charles R. Eiminhez, AIP Conference Procs. **177** (1988) 29.
- [5] J. Qiang, R.D. Ryne, S. Habib and V. Decyk: J. Comp. Phys. **163** (2000) 434.
- [6] V. Lebedev, Proceedings of 25th International Linear Accelerator Conference (LINAC10), Tsukuba, Japan, September 12 - 17, 2010. pp. 929 - 931.
- [7] Y. Liu et. al., Proceedings of 6th International Particle Accelerator Conference (IPAC15).